



Improvements to the BOLT Lightning Location System

Michael Stock, Ting Wu, Yasuhiro Akiyama, Tomoo Ushio, Zenichiro Kawasaki
Department of Electronic, Electromagnetic, and Information Engineering
Osaka University
Suita, Japan

Yoshitaka Nakamura
Department of Electrical Engineering
Kobe City College of Technology
Kobe, Japan

Michael Stock, Zenichiro Kawasaki
RAIRAN Pte. Ltd.
Kaizuka, Japan

Abstract—The Broadband Observational network for Lightning and Thunderstorms (BOLT) is a network of low frequency electric field antennas which is capable of mapping lightning flashes in 3D. We are currently investigating improvements to both the hardware design of the BOLT antennas, and to the algorithm used to determine each lightning source location. The antenna revision increases the sensitivity of the antenna to frequencies most beneficial to lightning location. The processing algorithm improvements have increased the number of lightning sources located, and produce 3D maps of sufficient quality for charge analysis.

Keywords—lightning; low-frequency; location; real-time

I. INTRODUCTION

The Broadband Observation network for Lightning and Thunderstorms (BOLT) is a network of 4 or more low frequency (LF) antennas deployed around the Kinki region of Japan. Currently, the array consists of 13 sensors deployed in a 90 km by 90 km region centered around Kobe (shown in Fig. 1). The data collected by the BOLT sensors can then be used to locate lightning sources in 3 spatial dimensions and time [1]. BOLT has successfully been used to detect and locate return strokes, K-processes, positive and negative upward leaders initiated from towners, preliminary breakdown, stepped leaders, and narrow bipolar events [2,3,4,5].

Each BOLT antenna consists of a flat plate antenna which senses the electric field convolved with a 157 μ s exponential decay. Such sensors are commonly used, and referred to as fast antennas. The signal is then passed through a 500 kHz low-pass filter to remove AM carrier noise, and digitized by a 4 MS/s, 14 bit digitizer in 200 ms records. The clock of each

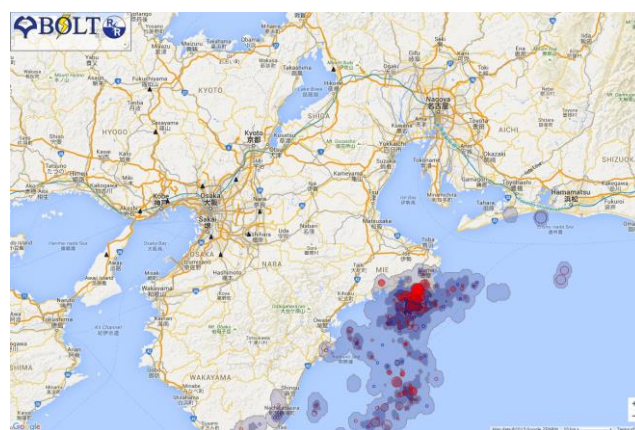


Figure 1. BOLT real-time display. Small black triangles indicate the location of sensor sites around the Kansai area of Japan. Lightning activity to the south-east of the network shows flash location, current, polarity, and extent density in an intuitive combined display.

digitizer is synchronized using GPS to better than 200 ns rms [1].

While lightning maps produced by BOLT are quite good in quality, we are still striving to further improve these locations. The improvements are proceeding along two directions: one is a hardware redesign of the front end amplifier; the other is improvements to the location algorithm. In this paper, we show the effects of these improvements.

II. HARDWARE IMPROVEMENTS

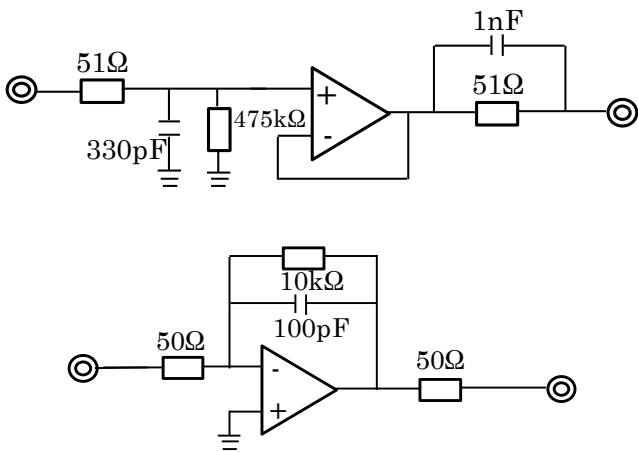


Figure 2. Top: Original circuit for the BOLT sensors with a 160 μ s time constant. Bottom: Redesigned DDT circuit with a 1 μ s time constant.

The current BOLT antenna design is simply a fast electric field change meter with a time constant of 157 μ s. A circuit diagram for the current BOLT antenna design is shown in fig. 2. This simple design has the advantage that signals recorded at the sensor are proportional to the electric field convolved with an exponential decay. This allows physical quantities such as peak current to be derived directly from the recorded signal.

Unfortunately, the current design also suffers from a number of weaknesses. We have found experimentally that frequency components below about 100 kHz do not add much to the location accuracy of the LF source. Yet, these frequency components account for the majority of the power recorded by the BOLT sensors. Noise contamination of the lowest frequency band can also be significant in the urban environment BOLT is deployed in.

To address these issues, a new amplifier design (shown in fig. 2) was proposed and referred to as the DDT antenna. The new circuit is based on a simple charge amplifier design, similar to that used in many fast electric field change sensors. Both the original BOLT and the DDT antennas sense the same physical quantity, electric field convolved with an exponential decay, but the time constant of the DDT antenna has been reduced to only 1 μ s. The effect of this is that for all frequencies within the BOLT sensing band (5-500 kHz), the electric field signal is differentiated with respect to time. This causes a linear increase in signal sensitivity with frequency, boosting the high frequencies and cutting the low frequencies, shown in fig. 3.

The new DDT antenna also corrected some minor design flaws of the original BOLT antenna. The DC impedance of the sensing plate was decreased from 475 k Ω with respect to ground (BOLT) to 50 Ω with respect to virtual ground (DDT). This means that the sensing plate for the DDT antenna always remains near ground potential. A voltage divider in the BOLT

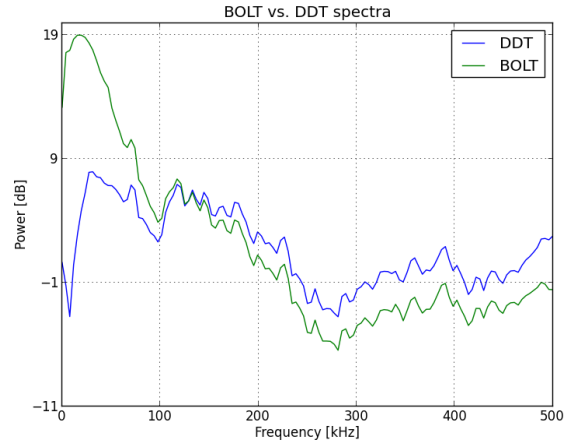


Figure 3. Frequency response of the original BOLT antenna, and the new DDT redesign. The new DDT antenna is less sensitive at frequencies lower than about 100 kHz, but more sensitive at frequencies above 100 kHz.

circuit was also removed, slightly increasing the signal amplitude of the DDT antenna.

Because the DDT antenna records dE/dt instead of ΔE like the BOLT antenna, the waveforms recorded by the two antennas do not look alike, as shown in fig. 4. As a consequence, the techniques used to estimate peak current from BOLT signals are not directly applicable to DDT signals. In addition, their unfamiliarity complicates identifying processes in the waveforms based on their shape. The difference in shape is drastic enough that a BOLT array using mixed antennas may suffer reduced accuracy or sensitivity. To alleviate these

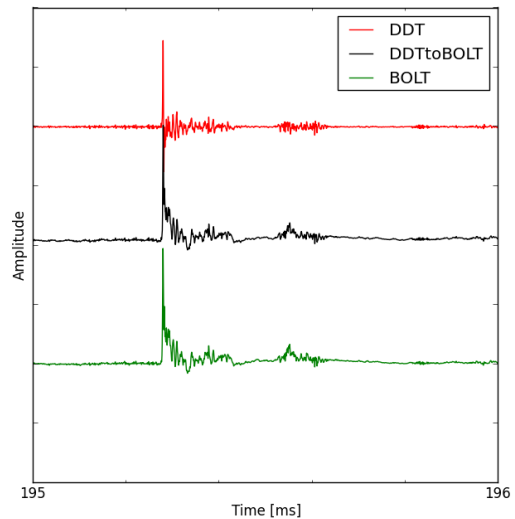


Figure 4. The time differentiated signal from the DDT circuit can be converted into the signal measured with the original BOLT antenna using a digital filter. The agreement between the digitally converted DDT and BOLT signals is excellent.

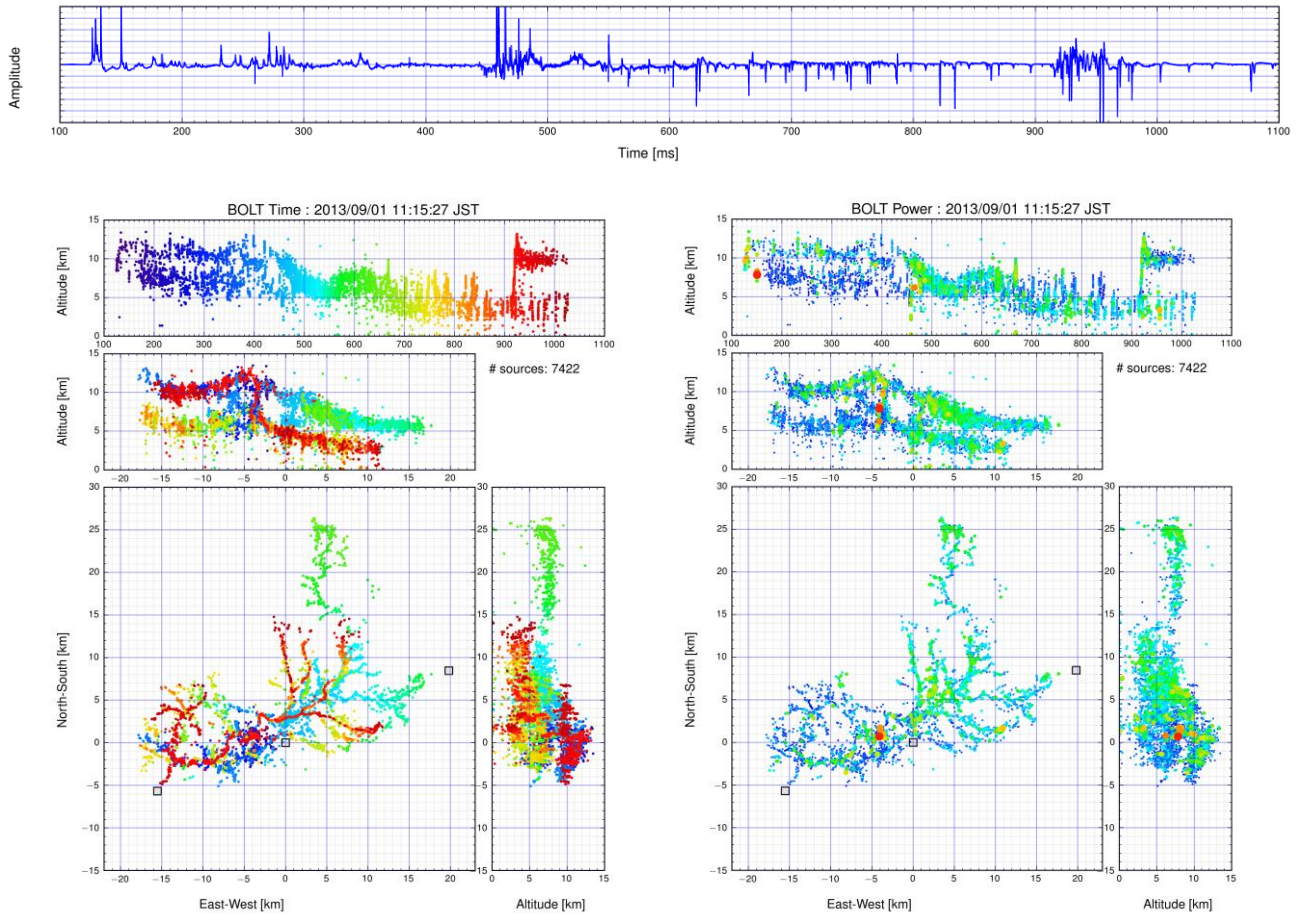


Figure 5. Example of improved BOLT mapping for a single IC flash. Top: time series electric field waveform record. Bottom: 3D maps of the LF lightning source locations colored by time (left) and estimated peak current (right). The 3D maps are shown in standard engineering format, displaying time-elevation, plan and vertical cross-sections.

problems, a digital filter was designed which converts a signal recorded by a DDT antenna to a signal recorded by a BOLT antenna, or vice versa. The results of this digital filter are very good, and shown in fig. 4. The DDT and BOLT waveforms in this figure were recorded by 2 independent antennas deployed about 3 m apart. After conversion, it is nearly impossible to identify differences between the waveforms, and peak current estimates from both are identical.

III. PROCESSING IMPROVEMENTS

In the past, BOLT produced 3D locations of lightning sources using a purely time-of-arrival (TOA) algorithm [1]. Recently, we have been experimenting with methods to improve upon those already very good results, and have developed both a hybrid TOA-Interferometric algorithm similar to [6], and a purely interferometric algorithm which produces images of the 3D coherence of the LF lightning signals. At this point, a full comparison of the different location algorithms has not been done. However, preliminary results suggest that both of the new algorithms locate substantially more LF sources than the previous TOA algorithm.

Fig. 5 shows the 3D map of a single lightning flash produced by the purely interferometric algorithm. Along the top is a time series of the electric field record recorded by one of the BOLT stations. On the bottom are the resulting 3D locations for the flash, in the standard LMA style view. The map on the left is colored by source time, showing the progression of the flash. The flash on the right is identical, but colored by estimated peak current for each located pulse using a standard transmission line model.

The flash shown in fig. 5 is a typical intra-cloud flash. The flash initiated with upward propagating preliminary breakdown pulses; negative breakdown. The initial leader then turns horizontal and continues extending. Activity can also be seen in the positive breakdown region a short delay after flash initiation. A delayed onset of activity in the positive breakdown region is a normal feature of VHF maps of lightning [7].

In the map shown in fig. 5, not only are the lightning channels delineated in the plan view, but the vertical accuracy is good enough to identify and isolate the positive and negative breakdown regions. This means we can employ charge

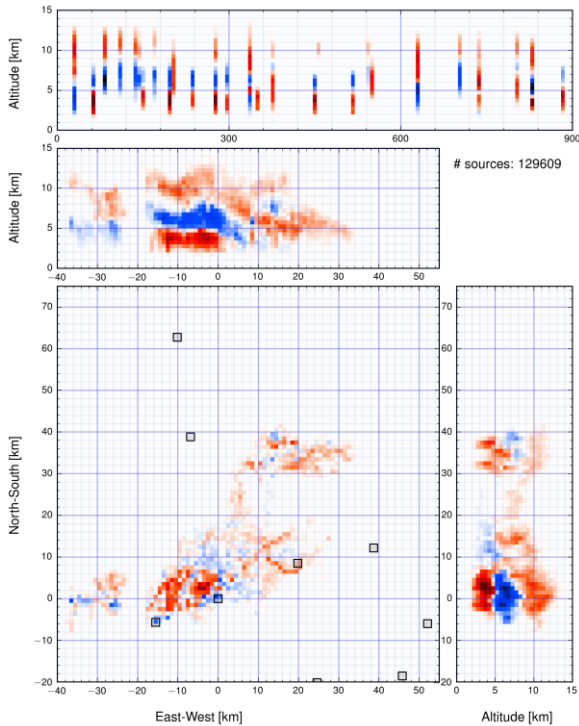


Figure 6. Charge analysis for a 15 minute period of BOLT lightning data. Blue (red) indicates regions of the cloud with inferred negative (positive) charge. This summer Japanese storm shows a typical tripolar structure.

analysis techniques like those of [8] using BOLT LF mapping data instead of data from a VHF mapping system. The results of charge analysis on a 15 minute segment of data are shown in fig. 6, blue regions show areas of negative charge and red regions show areas of positive charge. This summer storm over Japan shows a classic tripolar structure, similar to the charge structure seen in storms over New Mexico.

IV. CONCLUSIONS

We are making great progress in making improvements to both the hardware and processing algorithms of the already

well performing BOLT network. Evaluation of the new DDT antenna design is now complete, and it has been found to be performing exceptionally well. The less useful low frequency content has been filtered out, while improving the signal to noise ratio of the higher frequency components of the signal. This has been accomplished without sacrificing the capability of BOLT to estimate peak current, or measure time series electric field waveforms.

Qualitatively, the new BOLT processing algorithms are producing maps which rival those produced by VHF mapping systems. This means that high quality 3D mapping, return stroke location and identification, and current estimation are all possible using a single network of sensors.

Going forward, we plan to undertake a more in depth comparison of the different processing algorithms, and to do a wide scale deployment of the new DDT antennas.

- [1] Yoshida, S., T. Wu, T. Ushio, K. Kusunoki, and Y. Nakamura (2014), "Initial results of LF sensor network for lightning observation and characteristics of lightning emission in LF band", *J. Geophys. Res. Atmos.*, 119, 12,034–12,051
- [2] Takayanagi, T., M. Akita, Y. Nakamura, S. Yoshida, T. Morimoto, T. Ushio, and Z. Kawasaki (2012), "Leader process in 3D observed by VLF/LF broadband interferometer", the 31th International Conference on Lightning Protection, Austria, September 2012.
- [3] Takayanagi, Y., et al. (2012), "Upward lightning observed by LF broadband interferometer", *IEEJ Trans. Fundam. Mater.*, 133(3), 132–141.
- [4] Wu, T., S. Yoshida, Y. Akiyama, M. Stock, T. Ushio, and Z. Kawasaki (2015), "Preliminary breakdown of intracloud lightning: Initiation altitude, propagation speed, pulse train characteristics, and step length estimation", *J. Geophys. Res. Atmos.*, 120, 9071–9086
- [5] Wu, T., S. Yoshida, T. Ushio, Z. Kawasaki, and D. Wang (2014), "Lightning-initiator type of narrow bipolar events and their subsequent pulse trains", *J. Geophys. Res. Atmos.*, 119, 7425–7438
- [6] Lyu, F., S. A. Cummer, R. Solanki, J. Weinert, L. McTague, A. Katko, J. Barrett, L. Zigoneanu, Y. Xie, and W. Wang (2014), A low-frequency near-field interferometric-TOA 3-D Lightning Mapping Array, *Geophys. Res. Lett.*, 41, 7777–7784
- [7] M. Stock, M. Akita, P. Krehbiel, W. Rison, H. Edens, Z. Kawasaki, and M. Stanley (2014), "Continuous broadband digital interferometry of lightning using a generalized cross-correlation algorithm", *Journal of Geophysical Research: Atmospheres*, 119(6), 3134–3165.
- [8] Marshall, T. C., M. Stolzenburg, C. R. Maggio, L. M. Coleman, P. R. Krehbiel, T. Hamlin, R. J. Thomas, and W. Rison (2005), "Observed electric fields associated with lightning initiation", *Geophys. Res. Lett.*, 32, L03813